Glaucoma Diagnosis by Means of Optic Cup Feature Analysis in Color Fundus Images

Andres Diaz*, Sandra Morales*†, Valery Naranjo*†, Pablo Alcocer†‡ and Aitor Lanzagorta†‡
*Instituto de Investigación e Innovación en Bioingeniería, I3B,
Universitat Politècnica de València, Camino de Vera s/n, 46022 Valencia, Spain
Email: {andiapin,sanmomar,vnaranjo}@upv.es
†Grupo Tecnologías de Informática Aplicadas a la Oftalmología, Unidad Conjunta UPV- FISABIO, Spain
‡FISABIO Oftalmología Médica, 46015 Valencia, Spain

***Abstract*—Glaucoma is an asymptomatic eye disease and one of the major causes of irreversible blindness worldwide. For this reason, there have been significant advances in automatic screening tools for early detection. In this paper, an automatic glaucoma diagnosis algorithm based on retinal fundus image is presented. This algorithm uses anatomical characteristics such as the position of the vessels and the cup within the optic nerve. Using several color spaces and the Stochastic Watershed transformation, different characteristics of the optic nerve were analyzed in order to distinguish between a normal and a glaucomatous fundus. The proposed algorithm was evaluated on 53 images (24 normal and 29 glaucomatous images). The specificity and sensitivity obtained by the proposed algorithm are 0.81 and 0.87 using Luv color space, which means considerable performance in diagnosis systems.**

I. Introduction

Glaucoma is the second leading cause of blindness in the world [1]. In the literature, glaucoma is considered as a "multi factorial optic neuropathy" which affects 66.8 million people around the globe [2]. Intraocular pressure is usually an important aspect in glaucoma diagnosis. The increase of this pressure (IOP) may affect the optic nerve and may cause nerve damaged that involves loss of the retinal ganglion cells. Although the raised IOP is an important and modifiable risk factor for Glaucoma, it is not the only one. This means, there are people who have high eye pressure for a long time and the optic nerve is never affected. Glaucoma is also considered a silent eye-disease because it does not have symptoms until advance stages are reached. Since, no pain is associated with high IOP and glaucoma is asymptomatic in the early stages, its early detection and subsequent treatment is essential to prevent visual damage. Therefore, automated screening for glaucoma would be highly beneficial.

The optic disc (OD) is a round area in the back of the eye where retinal fibers are collected to form the optic nerve. This can be divided into two zones, a central bright zone called the cup and a peripheral region called the neuroretinal rim where the nerve fibers bend into the cup region [3]. As it is shown in the Fig. 1 .

The change in the optic nerve head in the presence of glaucoma is characterized by the increase of the cup size. This factor changes the appearance of the OD, as it is shown in Fig. 2(b). Typically, glaucoma detection is made by taking into account this deformation or "cupping" effect as well as the medical history, IOP and visual field loss test.

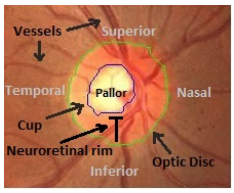

Fig. 1. Main structures of the optic disc region in a color fundus image

Since "cupping" effect is a important indicator of glaucoma progression, several characteristics of the optic disc region can be estimated using computer screening for early diagnosis. Characteristics such as cup to disc ratio or CDR that expresses the proportion of the disc occupies by the cup. It falls in the range of 0.3 to 0.5 for normal discs and for glaucomatous discs is higher than 0.5 [4]. Other characteristics are the area cup to disc ratio or ACDR that compares the optic nerve area with the cup area and the ISNT rule which determines a characteristic configuration for disc rim thickness. This rule is useful in evaluating whether the neuroretinal rim is normal or pathological. A normal neuroretinal rim tends to have the inferior part (I) thicker than the superior part (S) and the nasal part (N) thicker than the temporal part (T) (I >S >N >T) [5]. All these characteristics are quantitative and can help to track the glaucoma progression and classify images into normal and pathological eyes. Such characteristics can be obtained manually or by computer-based systems.

Many approaches have been developed towards the glaucoma detection in color fundus images, including level-set methods [6], superpixel classification [7], cup segmentation using r-bends information or vessel geometry and Hough transforms [8]. There was also developed a framework called ARGALI that measures automatically the cup to disc ratio (CDR).

This work focuses on glaucoma diagnosis using the CDR, ACDR and ISNT rule. In addition, a method for cup segmentation is proposed. This method analyses different color spaces and makes use of the Stochastic Watershed transformation.

978-0-9928-6265-7/16/$31.00 ©2016 IEEE

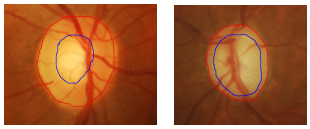

(a) (b)

Fig. 2. Difference between the aspect of the optic nerve in retinal fundus images: (a) Healthy optic nerve and (b) glaucomatous optic nerve.

II. Material

Two sets of images were used in this work. One of them, provided by 12 de Octubre Hospital (Madrid), is composed by 53 images of 768x576 pixels [9]. 30 of these images are classified as pathological and the remaining 23 as normal. The second set, DRIVE, is a public dataset composed by 40 images of 565x584 pixels [10]. In both datasets, the ground truth of the optic disc and the cup images are provided and obtained by specialists. Fig. 3

(a) (b) (c)

Fig. 3. Example of images used in the proposed automatic glaucoma diagnosis algorithm. (a) Original retinal color fundus image, (b) Ground truth of the OD and (c) Ground truth of the Cup.

III. Method

The complete flowchart of the glaucoma diagnosis algorithm is presented in Fig. 4. Each block will be described below.

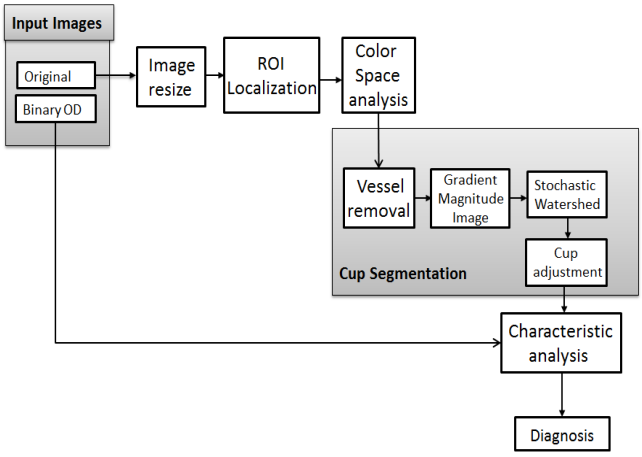

Fig. 4. Block diagram of the proposed glaucoma diagnosis algorithm

A. Image resize

Image resize is the first step of the algorithm. Due to the fact that the images under study belong to different databases, the image dimension varies. This block resizes the images to a standardized dimension in order to obtain comparable results. Images are resized using the length of the horizontal diameter of the fundus as reference [11]. Bicubic interpolation is used for resizing; the output pixel value is a weighted average of pixels in the nearest 4-by-4 neighborhood.

B. ROI localization

After image resize, the next step is to crop the image strategically. In this case, the algorithm crops the input images taking into account the center of the OD. OD masks were obtained based on the work presented in [12]. The algorithm takes about 10 more pixels, from the original image, surrounding the OD mask as it is shown in Fig.5 .

Fig. 5. Cropped image in the ROI, taking as reference the center of the optic disc.

C. Color Space analysis

Different color modes exist in the literature. In particular, color spaces tested in this work were RGB (Red Green and Blue components), CMYK (Cyan, Magenta, Yellow, and Key (black) components), PCA (Principal Component Analysis), YIQ (Used in NTSC color TV system) and XYZ, Lab and Luv which were created by the International Commission on Illumination (CIE).

A first analysis of these color spaces was made in order to check which one has the best performance in cup segmentation.

It was found that components with better performance were component “v” in color space Luv, second component in PCA, Cyan and Key components in CMYK and “Q” component in YIQ color space. They are shown in Fig. 6 .

It is possible to see that the cup is usually darker or brighter than the other part of the image. The proposed algorithm is basically based on that. Supposing an image as a topographic surface where the cup can be the lowest or the highest part of that surface. Quantitative results of the classification and when these color space components were used for cup segmentation will be presented in section IV.

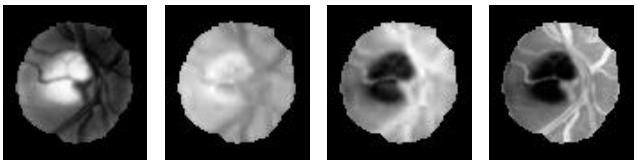

(a) (b) (c) (d)

Fig. 6. Different color spaces components used as input to the developed algorithm. (a) Second PCA component, (b) **v** in Luv space, (c) **Q** in YIQ space and (d) **C+K** components in CMYK space.

D. Cup Segmentation

Cup segmentation block is divided in 3 main parts. Vessel removal, Stochastic Watershed method and the Cup adjustment block.

1) Vessel removal: Vessel removal is performed using an inpainting technique [13]. In particular, a simple diffusion-based algorithm was implemented, which fills vessel spaces by diffusing the image information from the known region at pixel level [14]. An example of this is shown in Fig. 7 (c).

For vessel segmentation procedure, a method based on mathematical morphology and curvature evaluation was used [15].

2) Stochastic Watershed Segmentation: Watershed transformation [16] is the segmentation technique used in this work. Watershed transformation was developed for gray-scale images. This algorithm is a powerful segmentation technique whenever the minima of the image represent the objects of interest and the maxima are the separation boundaries between objects. For that reason, the input image of this transformation is usually the gradient image.

In mathematical morphology, the gradient of an image is obtained as the pointwise difference between a unitary dilation and a unitary erosion. A gradient image example is shown in Fig. 7 (d).

One problem of this technique is the over-segmentation, which is caused by the existence of numerous local minima in the image due to the presence of noise. This problem is solved establishing the image minima artificially, defining a marker per minimum. In this work, regionalized random markers were used. This means, non-uniform random markers whose distribution is restricted to areas that accomplished a specific condition. In this work, they can only be located in low-intensity areas. These intensity regionalized markers follow a Poisson distribution with variance σ^2 [17] . Fig.7 (e). In this transformation, a given number M of marker-controlled watershed realizations are performed selecting N pseudo-random markers in each realization. The idea is to estimate a probability density function (pdf) for the countours of the image, which filter out non-significant border fluctuations. The probability density function is computed by Parzen window method [18] as follows:

$$pdf(\mathbf{x}) = \frac{1}{M}\sum_{i=1}^{M}(WS_i(\mathbf{x}) * G(\mathbf{x}; s)) \qquad (1)$$

where $G(\mathbf{x}; s)$ represents a Gaussian function of variance σ^2 and mean $\mu(\mu = 0)$, M the sets of N regionalized random markers and $WS_i = WS(\varrho)_{f_{mrk_i}}$ the ith output watershed image, being ϱ the gradient image. Fig. 7 (f) illustrates how the pdf is. Afterwards, it is necessary to perform a last marker-controlled watershed transformation on the pdf, which defines the resulting mask by joining all the watershed regions.

Fig. 7 shows different intermediate and final results of the Stochastic Watershed algorithm.

Fundamentally, this is the neuralgic step in the proposed algorithm. Therefore, the variable parameters of the watershed algorithm were carefully analyzed (the variance of the Poisson function that generates the random markers and the number of random markers). The variance σ^2 was set in 0.0003 up to 0.01, the number of markers were set between the range $10-15$ up to the range $400-500$ and the number of realizations was set in 5. The random markers are limited by the region of interest of the image. For that reason, they are not completely random. This limitation makes them pseudo-random markers. In order to obtain optimum values, several tests were carried out. The results of these tests are shown in Section IV .

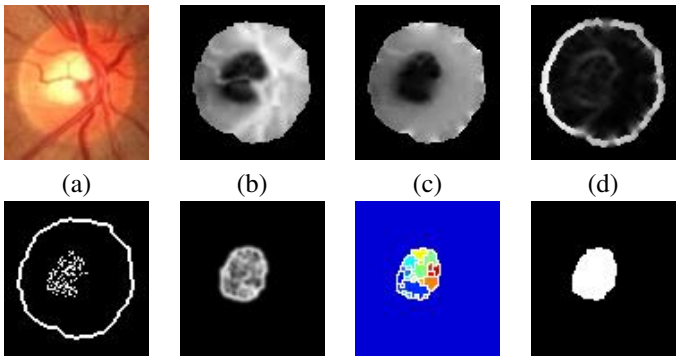

Fig. 7. Process of the Stochastic Watershed: (a) image region of interest, (b) Gray-level image (Q component in YIQ color space), (c) vessel removal, (d) Gradient image, (e) Pseudo-random markers, (f) *pdf* of image contours, (g) Watershed regions and (h) Final generated mask.

3) Cup adjustment: The cup adjustment block is basically implemented to improve the performance in measuring CDR and ISNT.

Firstly, it is calculated the total area of the mask obtained by the Stochastic Watershed method, which is based on the pallor that characterizes the cup. Secondly, it is generated a circle with the same area of the generated Stochastic Watershed mask and is placed in the center of the optic disc. With this adjustment, the cup segmentation takes into account the geometrical cup position, which is, most of the cases, where the vessels exit to the retina.

In Fig. 8 cup adjustment result is shown. In this figure the white and green lines identify the optic disc and cup, respectively (segmentation made by specialists). The yellow line represents the segmentation using pure Stochastic Watershed method and the blue line represents the adjustment made to the segmented cup.

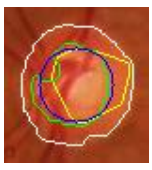

Fig. 8. Image result of the cup adjustment block

E. Glaucoma Diagnosis

The proposed method for cup segmentation is used to measure characteristics such as CDR, ACDR and ISNT rule,

which are helpful in the glaucoma diagnosis. Therefore, it is important to define how these measurements were calculated.

ACDR is the ratio between the cup area and the optic disc area. In [5], CDR is defined as the proportion of the optic disc that is occupied by the cup. This proportion is typically measured as the ratio of the vertical diameter of the cup and the vertical diameter of the optic disc. Regarding to the ISNT rule, the vertical and horizontal thickness of the optic nerve rim are measured. The vertical thickness represents the inferior part (I) plus the superior part (S) of the neuroretinal rim: VerDiam $= I + S$, and the horizontal thickness represents the temporal part (T) plus the nasal part (N) of the neuoretinal rim: HorDiam $= I + S$. If the vertical thickness is higher than horizontal diameter, the image is classified as "Normal", otherwise it is classified as "Glaucomatous".

Due to the fact that the shape of the OD and the cup is not completely regular, the proposed algorithm calculates the CDR computing the diameter of the optic disc and the cup, as the mean of the two highest vertical diameters.

In order to establish optimum thresholds for glaucoma diagnosis, 10-fold cross validation was used on 12Octubre dataset. The obtained threshold for the CDR and the ACDR were 0.56 and 0.30 respectively.

IV. Results

12Octubre and DRIVE datasets were used to test the performance of the proposed algorithm. Both datasets were used to check the performance of the proposed cup segmentation method. On the other hand, given 12Octubre dataset is divided into normal and glaucomatous eye, but DRIVE is not; only 12Octubre dataset was used to analyze the performance of the algorithm in glaucoma diagnosis. In this section quantitative results will be shown for each analysis.

A. Cup Segmentation Results

In this section, the performance comparison between five color spaces in cup segmentation using the Stochastic Watershed method is shown: CMYK, YIQ, Luv, Lab and PCA. Specifically component "C" plus component "K" in CMYK, component "Q" in YIQ, component "v" in Luv, component "a" in Lab and second component in PCA color space. This comparison was made using DRIVE and 12Octubre datasets and calculating the Jaccard and Dice indexes between the ground truth masks and the segmentation results. Different Jaccard and Dice indexes were obtained using as inputs each aforementioned color components. The aim of this test is to determine the best gray image that can be used as input of our method.

This comparison was conducted by running several times the algorithm with different settings, such as the variance of the function that generates the pseudo-random markers and the number of pseudo-random markers in the Stochastic Watershed method. The optimum values of the variance (σ^2) for each color space are shown in Table I. All these results were obtained using a minimun 100 and maximum of 130 random markers. As it is shown in Fig. 9 (a), it was found that increasing or decreasing the number of random markers the performance of the Stochastic Watershed method decreases and then, the performance of the algorithm.

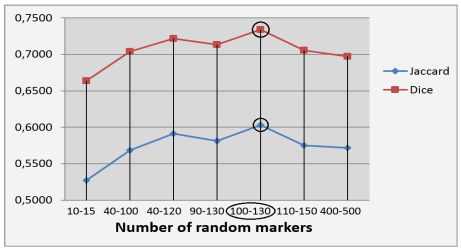

(a)

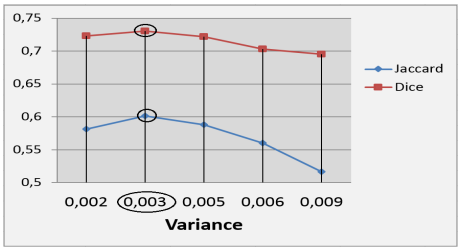

(b)

Fig. 9. Cup segmentation analysis using CMYK color space: (a) Results for different number of random markers ($\sigma^2 = 0.003$) and (b) Results for different variance values (using 100 to 130 pseudo-random markers).

Table I also shows the difference between the performance obtained by using only the Stochastic Watershed method and the performance obtained using cup adjustment block. Cup segmentation results for each color space were obtained using the same values, shown in Table I, for the variance and number of random markers (between 100 to 130). These results are represented by means of the True Positive Factor (TPF_mean) and the False Positive Factor (FPF_mean). These measurements represent, in this case, sensitivity and specificity for each image at pixel level.

From the obtained results in Table I , it is observed that CMYK, YIQ and Luv color spaces show higher specificity and sensitivity values in comparison to Lab and PCA color spaces. This implies higher performance in glaucoma diagnosis.

B. Specificity and Sensitivity in Glaucoma Diagnosis

In Table II , specificity and sensitivity for glaucoma diagnosis obtained by different color spaces are shown. These results were obtained using the cup adjustment block. CDR, ACDR and ISNT rule are evaluated using the same five color spaces, as it was shown in Table II.

From these results, it is observed that the best performance in glaucoma diagnosis is obtained by the Luv color space using the CDR. However, CMYK and YIQ color spaces show considerable values of specificity and sensitivity, which means reliable glaucoma diagnosis results.

V. Conclusions and Further Work

In this paper, an automatic glaucoma diagnosis algorithm that uses the Stochastic Watershed transformation to segment the cup from digital color fundus images was proposed. With

TABLE I
COLOR SPACE ANALYSIS RESULTS SHOWING CUP ADJUSTMENT EFFECTS.

	Without Cup adjustment					With Cup adjustment				
	CMYK	**YIQ**	**Luv**	**Lab**	**PCA**	**CMYK**	**YIQ**	**Luv**	**Lab**	**PCA**
σ^2	0.003	0.025	0.003	0.035	0.020	0.003	0.025	0.003	0.035	0.020
J_mean	0,5076	0,4867	0,5095	0,5095	0,4898	**0,6027**	**0,6062**	**0,5991**	0,5858	0,5212
D_mean	0,6410	0,6218	0,6418	0,6404	0,6333	**0,7339**	**0,7398**	**0,7281**	0,7187	0,6659
TPF_mean	0,6764	0,6078	0,7140	0,8738	0,6409	0,8503	0,8046	0,8759	0,6931	0,6107
FPF_mean	0,0023	0,0018	0,0033	0,0057	0,0019	0,0030	0,0020	0,0040	0,0012	0,0011

TABLE II
GLAUCOMA GIAGNOSIS USING CDR, ACDR AND ISNT RULE THROUGH CMYK, YIQ, LUV, LAB AND PCA COLOR SPACES

	CMYK		**YIQ**		**Luv**		**Lab**		**PCA**	
	Specificity	**Sensitivity**	**Specificity**	**Sensitivity**	**Specificity**	**Sensitivity**	**Specificity**	**Sensitivity**	**Specificity**	**Sensitivity**
CDR	0,8333	0,7845	0,8438	0,6552	**0,8125**	**0,8707**	0,9583	0,6207	0,7292	0,6724
ACDR	0,7396	0,8793	0,7708	0,6724	0,7292	0,9483	0,8438	0,6207	0,6458	0,6724
ISNT	0,6875	0,5517	0,7083	0,5086	0,6771	0,4828	0,7083	0,5259	0,7083	0,4655

this algorithm, a complete performance analysis of five color spaces: CMYK, YIQ, Luv, lab and PCA was shown. From this analysis, the use of CMYK, YIQ and Luv color spaces shown higher specificity and sensitivity results for cup segmentation. After that, several known characteristics such as CDR, ACDR and ISNT rule were measured. From the computed CDR by using Luv color space and the Cup adjustment block, a specificity of 0.8125 and sensitivity of 0.8707 for glaucoma diagnosis were obtained.

Future work will focus on other techniques such as dictionary learning, texture analysis and superpixel classification for glaucoma diagnosis.

ACKNOWLEDGMENT

This work was supported by the Ministerio de Economía y Competitividad of Spain, Project ACRIMA (TIN2013-46751-R). The work of Andres Diaz has been supported by the Generalitat Valenciana under the scholarship Santiago Grisolia (GRISOLIA/2015/027). The authors would like to thank to the Department of Ophthalmology of the Hospital 12 de Octubre de Madrid (Spain) and to the Department of Electronics of the Universidad de Alcalá (Spain) for facilitating access to their database.

REFERENCES

[1] "Bulletin of the world health organization," http://www.who.int/bulletin/volumes/82/11/feature1104/en/, Accessed: 2016-01-14.

[2] R R A Bourne, "Worldwide glaucoma through the looking glass," in *British Journal of Ophthalmology*, 2006, pp. 253–254.

[3] R. Bock, J. Meier, L. G. Nyúl, J. Hornegger, and G. Michelson, "Glaucoma risk index: Automated glaucoma detection from color fundus images," *Medical Image Analysis*, vol. 14, no. 3, pp. 471–481, June 2010.

[4] M. K. Nath and S. Dandapat, "Techniques of glaucoma detection from color fundus images: A review," *I.J. Image, Graphics and Signal Processing*, 2012.

[5] "optic-disc.org, an online resource for ophthalmologists, physicians, medical students and optometrists," http://www.optic-disc.org/tutorials/glaucoma_evaluation_basics/page13.html, Accessed: 2016-01-18.

[6] D. W. K. Wong, J. Liu, J.H. Lim, X. Jia, F. Yin, H. Li, and T. Y. Wong, "Level-set based automatic cup-to-disc ratio determination using retinal fundus images in ARGALI," in *30th Annual International IEEE EMBS Conference*, Vancouver, British Columbia, Canada, 2008.

[7] J. Cheng, J. Liu, Y. Xu, F. Yin, D. W. K. Wong, N. Tan, D. Tao, C. Cheng, T. Aung, and T. Y. Wong, "Superpixel classification based optic disc and optic cup segmentation for glaucoma screening," *IEEE TRANSACTIONS ON MEDICAL IMAGING*, vol. 6, no. 32, 2013.

[8] G. D. Joshi, J. Sivaswamy, and S. R. Krishnadas, "Optic disk and cup segmentation from monocular color retinal images for glaucoma assessment," *IEEE TRANSACTIONS ON MEDICAL IMAGING*, vol. 30, no. 6, 2011.

[9] R. Morán, R. Barea Navarro, L. Boquete Vázquez, E. López Guillén, J. Campos Pavón, L. de Pablo Gómez de Liaño, D. Escot Bocanegra, L. de Santiago, and M. Ortiz, "Color analysis in retinography: Glaucoma image detection," in *XIII Mediterranean Conference on Medical and Biological Engineering and Computing 2013*, vol. 41 of *IFMBE Proceedings*, pp. 325–329. 2014.

[10] "Drive: Digital retinal images for vessel extraction," http://www.isi.uu.nl/Research/Databases/DRIVE/, Accessed: 2016-01-14.

[11] X. Zhang, G. Thibault, E. Decencière, G. Quellec, G. Cazuguel, A. Erginay, P. Massin, and A. Chabouis, "Spatial normalization of eye fundus images," in *ISBI 2012: 9th IEEE International Symposium on Biomedical Imaging*, 2012.

[12] S. Morales, V. Naranjo, J. Angulo, and M. Alcañiz, "Automatic detection of optic disc based on PCA and mathematical morphology," *IEEE Transactions on Medical Imaging*, vol. 32, no. 4, pp. 786–796, April 2013.

[13] M. Bertalmio, G. Sapiro, V. Caselles, and C. Ballester, "Image inpainting," *Proceedings of the 27th annual conference on Computer graphics and interactive techniques*, 2000.

[14] Sonal Bhangale and A. N. Shaikh, "Image inpainting," in *International Journal of Engineering and Innovative Technology (IJEIT)*, 2012.

[15] S. Morales, V. Naranjo, J. Angulo, J. J. Fuertes, and M. Alcañiz, "Segmentation and analysis of retinal vascular tree from fundus images processing," in *International Conference on Bio-inspired Systems and Signal Processing (BIOSIGNALS 2012)*, 2012, pp. 321 – 324.

[16] S. Beucher and F. Meyer, *Mathematical Morphology in Image Processing*, New York: Marcel Dekker, 1992.

[17] J. Angulo and D. Jeulin, "Stochastic watershed segmentation," in *Proceedings of the 8th International Symposium on Mathematical Morphology*, Rio de Janeiro, Brazil, 2007, pp. 265–276.

[18] R. O. Duda, P. E. Hart, and D. G. Stork, *Pattern Classification and Scene Analysis (2nd ed.)*, John Wiley & Sons, 1995.